

Current Topics

Revealing the Nature of the Native State Ensemble through Cold Denaturation[†]

Steven T. Whitten,[‡] Andrew J. Kurtz,[‡] Maxim S. Pometun,[§] A. Joshua Wand,^{*,§} and Vincent J. Hilser^{*,‡}

Department of Biochemistry and Molecular Biology and Sealy Center for Structural Biology and Molecular Biophysics, University of Texas Medical Branch, Galveston, Texas 77555-1055, and Johnson Research Foundation and Department of Biochemistry and Biophysics, University of Pennsylvania, Philadelphia, Pennsylvania 19104-6059

Received May 1, 2006; Revised Manuscript Received July 21, 2006

ABSTRACT: Recent advances in NMR methodology have enabled the structural analysis of proteins at temperatures far below the freezing point of water, thus opening a window to the cold denaturation process. Although the phenomenon of cold denaturation has been known since the mid-1970s, the freezing point of water has prevented detailed and structurally resolved studies without application of additional significant perturbations of the protein ensemble. As a result, the cold-denatured state and the process of cold denaturation have gone largely unstudied. Here, the structural and thermodynamic basis of cold denaturation is explored with emphasis placed on the insights that are uniquely ascertained from low-temperature studies. It is shown that the noncooperative cold-induced unfolding of protein results in the population of partially folded states that cannot be accessed by other techniques. The structurally resolved view of the cold denaturation process therefore can provide direct access to the cooperative substructures within the protein molecule and provide an unprecedented structurally resolved picture of the states that comprise the native state ensemble.

The protein folding equilibrium is often described as a two-state process in which the folded native state is in equilibrium with an unfolded or denatured state. This depiction arose out of early protein folding studies in which temperature was used to promote the structural transition from the native state to the thermally denatured or heat-denatured state, and it was well-established that the transition could be empirically described in terms of a simple two-

state process (1, 2). Although the two-state view of proteins persists, it does not reflect the situation under strongly native conditions, where both hydrogen exchange (3–10) and NMR relaxation (11–13) studies reveal significant conformational heterogeneity. Such studies indicate that under native conditions, a protein has access to a remarkably rich conformational manifold and that excursions across this manifold are important for a range of biological functions, particularly for establishing a basis for catalysis and site-to-site communication. Unfortunately, little about the detailed structure and energy of the myriad of near-native states is known. This is due in part to the fact that under native conditions, each of the individual conformational (micro) states contributes only minutely to the overall observed properties, and there is considerable difficulty in experimentally resolving the contributions from these different states. Thus, a structurally resolved view of the conformational heterogeneity of a

[†] Supported by NIH Grants GM 13747 (V.J.H.) and GM 35940 (A.J.W.) and Robert A. Welch Foundation Grant H-1461 (V.J.H.). A.J.K. is supported by the Jeane B. Kempner Fund.

* To whom correspondence should be addressed: Department of Biochemistry and Biophysics, University of Pennsylvania, 905 Stellar-Chance Labs, 422 Curie Blvd., Philadelphia, PA 19104-6059. Telephone: (215) 573-7288. Fax: (215) 573-7290. E-mail: vjhilser@utmb.edu or wand@mail.med.upenn.edu.

[‡] University of Texas Medical Branch.

[§] University of Pennsylvania.

protein, as well as a corresponding structure-based thermodynamic description that can relate the measured properties with the individual conformations, represents a cornerstone to a quantitative thermodynamic understanding of the native state ensemble.

Recently, we took advantage of the seemingly unrelated phenomena of cold denaturation to provide a comprehensive and structurally resolved picture of the energy landscape of ubiquitin (14). The unique insights provided by cold denaturation stem from the Gibbs–Helmholtz equation describing the temperature dependence of a thermodynamic equilibrium. From the formal definitions of the temperature dependence of the changes in system enthalpy (ΔH) and entropy (ΔS):

$$\Delta H(T) = \Delta H(T_{\text{ref}}) + \int \Delta C_p dT \quad (1)$$

and

$$\Delta S(T) = \Delta S(T_{\text{ref}}) + \int \frac{\Delta C_p}{T} dT \quad (2)$$

a familiar form of the Gibbs–Helmholtz expression can be obtained through integration, with the assumption of a temperature-independent change in heat capacity (ΔC_p) and substitution of a common reference temperature (T_{ref}):

$$\Delta G(T) = \Delta H(T_{\text{ref}}) + \Delta C_p(T - T_{\text{ref}}) - T[\Delta S(T_{\text{ref}}) + \Delta C_p \ln(T/T_{\text{ref}})] \quad (3)$$

As is well-known, positive values of ΔC_p produce a curvature in the free energy function, which leads to a distinct maximum of the free energy profile for each state; the high heat capacity of unfolded states relative to more folded ones thus promotes a transition to these states at both high and low temperatures. Interestingly, however, cold denaturation does not occur in the cooperative fashion that characterizes the thermal denaturation process. Instead, cold denaturation is noncooperative (15, 16), and as we will show, a structurally resolved view of the states that become populated during the cold denaturation process provides an unparalleled glance at the structural features of the conformational fluctuations that dominate the native state ensemble.

Here we investigate the unique structural and thermodynamic information that may be obtained about the native state ensemble from the process of cold denaturation. We start with a phenomenological investigation of the origins of cooperativity for protein folding–unfolding processes, using a simple hierarchical cooperative model. This model demonstrates the origins of noncooperative cold denaturation and cooperative heat denaturation. Next, we show how the experimentally observed cold denaturation of ubiquitin provides unique insights about the nature of the partially folded states in a protein's conformational manifold. Finally, we show that a structure-based ensemble model, in which the conformational excursions are modeled in a manner consistent with the experimentally observed features, predicts the experimentally observed noncooperative cold denaturation, as well as the structural features of the cold-denatured states. The self-consistent view of the native state ensemble that emerges from this analysis provides unique insights into

the challenges associated with characterizing protein fluctuations and evaluating their impact on function.

Connecting Cold Denaturation to the Native State Ensemble Using Hierarchical Protein Models

To understand the difference between the information that is obtained from cold versus thermal denaturation studies, we employ a hierarchical model of proteins described previously by Brandts and Lin (17), Murphy and Freire (18), and Hilser et al. (19). Within the context of this construct, a protein can be considered as being composed of any number of independent structural units or domains, which can interact with one another (Table 1). The simplest situation is a two-domain protein, wherein each domain can unfold in a manner independent of one another, but which can also interact through a hypothetical common surface. This model is considered hierarchical because the overall behavior of the protein is dependent on the energetics of the individual domains as well as the interaction energy between them. As demonstrated below, the transition from the native to the fully unfolded state can range from entirely cooperative to entirely noncooperative, proceeding through the accumulation of intermediate states in which one domain is folded and the other is unfolded.

Dissection of the two-domain protein reveals the origins of cooperativity. There are four states accessible to the system, including two possible intermediates (Table 1). Differences in the cooperativity of unfolding arise because the free energy of each state is comprised of the intrinsic stabilities of the individual domains (i.e., ΔG_1 and ΔG_2) as well as the interaction energies between them (i.e., Δg_{int}). The corresponding partition function for this system, Q , which is simply the sum of the statistical weights of the accessible states accessible, is

$$Q = 1 + K_1\phi + K_2\phi + K_1K_2\phi \quad (4)$$

where $K_1 = \exp(-\Delta G_1/RT)$, $K_2 = \exp(-\Delta G_2/RT)$, and $\phi = \exp(-\Delta g_{\text{int}}/RT)$. Cooperativity in this system arises as a result of the interaction parameter between the domains, ϕ . In the case where $\phi = 1$ (i.e., $\Delta g_{\text{int}} = 0$), there is no interaction and the partition function reduces to that for two independent domains. In other words, the energy of unfolding both domains is simply the sum of unfolding energies of the individual domains, and the stability of one domain is uncoupled from the stability of the other. Thus, from a mathematical perspective, cooperativity arises when $\Delta g_{\text{int}} \neq 0$. In such a case, the degree of cooperativity will be determined by the relative magnitude of the three parameters in eq 4. When Δg_{int} is large and positive, disrupting the interaction between the two domains is relatively unfavorable (see Figure 1). As a result, the native structure will remain intact until such conditions of temperature (or pH, denaturant concentration, etc.) where the combined intrinsic instabilities of both domains overcome the unfavorable energy involved in breaking the interaction between subunits. That is, when Δg_{int} is large, the interaction will not be disrupted until such conditions where the ΔG for the domains is equally large and negative. Since this means, by definition, that the individual units are unstable, the intermediates depicted in Table 1 will not be populated to a significant extent during the transition. Under these conditions, the native and

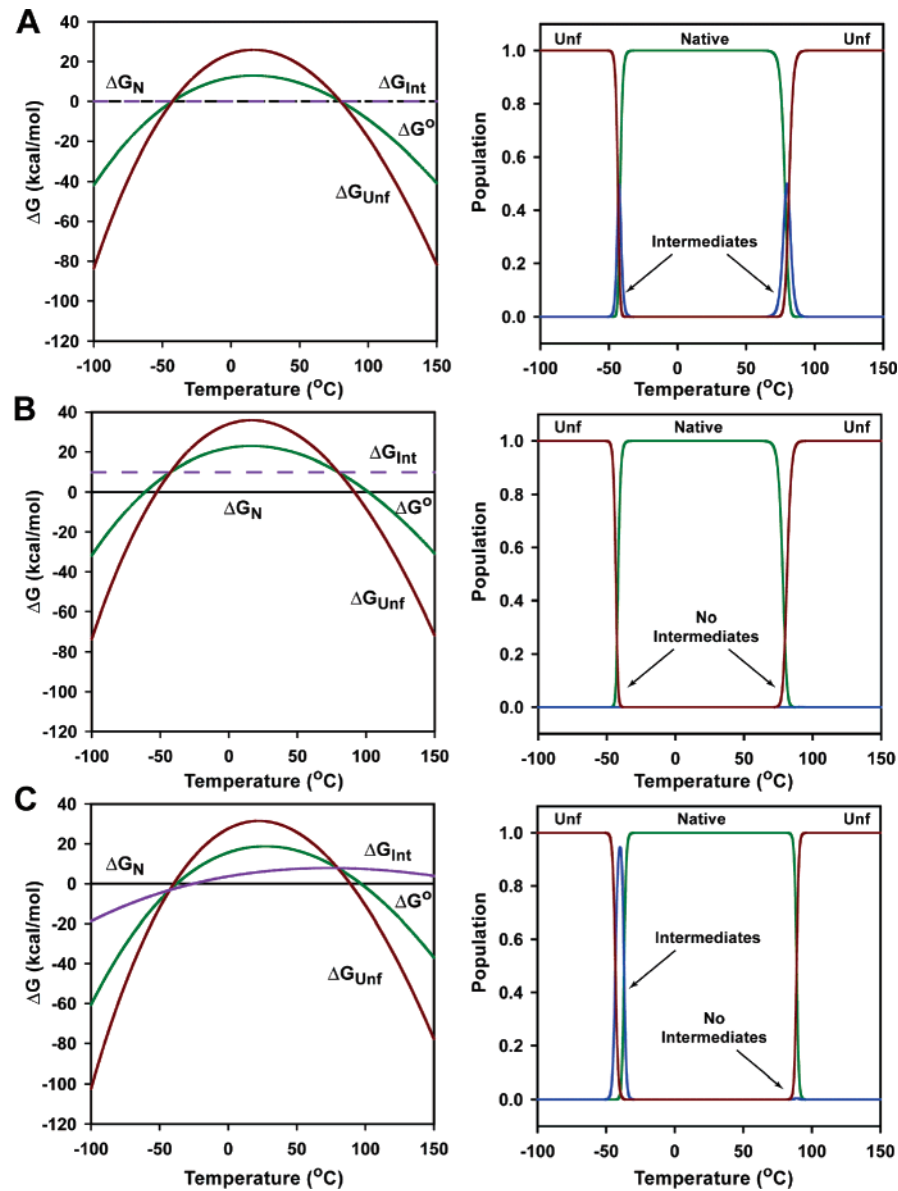


FIGURE 1: Simulated temperature dependence of the two subglobal unit system, as defined in Table 1. Each subglobal unit was given the intrinsic thermodynamic parameters of a typical globular protein (26). All simulations used the following: $\Delta H^\circ(60^\circ\text{C}) = \Delta H_1 = \Delta H_2 = 100\text{ kcal/mol}$, $\Delta S^\circ(60^\circ\text{C}) = \Delta S_1 = \Delta S_2 = 280\text{ cal K}^{-1}\text{ mol}^{-1}$, and $\Delta C_p^\circ = \Delta C_{p,1} = \Delta C_{p,2} = 2\text{ kcal K}^{-1}\text{ mol}^{-1}$. The interaction energy between the subglobal units, Δg_{int} , was modeled as (A) a temperature-independent value of 0 kcal/mol, (B) a temperature-independent value of 10 kcal/mol, and (C) a temperature-dependent value calculated from a $\Delta H_{\text{int}}(60^\circ\text{C})$ of 1 kcal/mol, a $\Delta S_{\text{int}}(60^\circ\text{C})$ of $-20\text{ cal K}^{-1}\text{ mol}^{-1}$, and a $\Delta C_{p,\text{int}}$ of $0.5\text{ kcal K}^{-1}\text{ mol}^{-1}$ using the relation $\Delta g_{\text{int}}(T) = \Delta H_{\text{int}}(T) - T\Delta S_{\text{int}}(T)$. Shown for each group (A–C) are the relative free energy, ΔG , of the system and the relative probability of each state.

Table 1: Schematic Representation of the States, Relative Free Energies, and Statistical Weights for a Two-Subglobal Unit Protein









State	Free Energy	Statistical Weight
	0	1
	$\Delta G_1 + \Delta g_{\text{int}}$	$K_1\phi$
	$\Delta G_2 + \Delta g_{\text{int}}$	$K_2\phi$
	$\Delta G_1 + \Delta G_2 + \Delta g_{\text{int}}$	$K_1K_2\phi$

completely unfolded states are the only thermodynamically relevant states, and the transition will be highly cooperative (i.e., two-state). Similarly, intermediate levels of folding—

unfolding cooperativity arise from conditions in which Δg_{int} is relatively small compared to the intrinsic stability of one or both domains.

In Figure 1, quantitative simulations have been performed to demonstrate the relationships described above for the two-domain system. In these simulations, a range of interaction free energies (Δg_{int}) were applied, keeping the intrinsic free energy of each subdomain constant (ΔG° , where $\Delta G^\circ = \Delta G_1 = \Delta G_2$). Importantly, when the thermodynamic parameters for Δg_{int} were set to values consistent with the nonspecific burial of hydrophobic surface upon interaction between the two subglobal units (20), the temperature dependence of Δg_{int} is observed to vary such that the interaction between the two domains is favorable at high temperatures yet unfavorable at low temperatures. This temperature dependence of the interaction energy, which can be inferred directly from

Table 2. Schematic Representation of the States, Relative Free Energies, and Statistical Weights for a Four-Subglobal Unit Protein^a

	State	Free Energy	Statistical Weight
N		0	1
1		$\Delta G^\circ + 2\Delta g_{\text{int}}$	$2K^\circ\phi^2$
2		$\Delta G^\circ + 2\Delta g_{\text{int}} + \Delta g_{\text{close}}$	$2K^\circ\phi^2\phi_{\text{close}}$
3		$2\Delta G^\circ + 3\Delta g_{\text{int}} + \Delta g_{\text{close}}$	$3K^\circ\phi^3\phi_{\text{close}}$
4		$2\Delta G^\circ + 3\Delta g_{\text{int}}$	$K^\circ\phi^3$
5		$2\Delta G^\circ + 4\Delta g_{\text{int}} + \Delta g_{\text{close}}$	$2K^\circ\phi^4\phi_{\text{close}}$
6		$3\Delta G^\circ + 4\Delta g_{\text{int}} + \Delta g_{\text{close}}$	$4K^\circ\phi^4\phi_{\text{close}}$
UNF		$4\Delta G^\circ + 4\Delta g_{\text{int}} + \Delta g_{\text{close}}$	$K^\circ\phi^4\phi_{\text{close}}$

^a Each subunit has an intrinsic stability of ΔG° and interacts with neighboring subunits through the interaction energy, Δg_{int} , and the two end subunits (units 1 and 4) interact with additional entropy derived closure energy, Δg_{close} , representing loop formation. Unfolded subunits are represented as blue circles, whereas the white circles represent the folded subunits.

transfer free energy measurements (21), is the reason for the cooperative heat denaturation and noncooperative cold denaturation. Thus, the very simple hierarchical model described here provides a means of reconciling the experimentally observed differences in the cooperativity between thermal and cold denaturation, as well as providing a mechanistic reason for the observed differences.

Extending the Hierarchical Model To Investigate the Nature of Cold-Induced Intermediates

The hierarchical model can be extended to any number of domains or independently folding elements. In an effort to illuminate potentially more subtle trends and to provide insight into the cold-denatured intermediates, the model was extended to include four interacting units. This slightly more complex system is sufficiently large to convey additional phenomena yet small enough to consider each state explicitly without becoming intractable. For this model, the four subunits (domains) each have an intrinsic statistical weight, K° , and are considered to be ordered sequentially in a chain (Table 2). Each subunit interacts with its neighboring subunits through the parameter ϕ , and the two end subunits interact with an additional entropy term for closing the chain into a loop. The relative free energies and the statistical weights of each state are listed in Table 2. To distinguish different classes of intermediates, all states that are energetically equivalent were grouped.

Like the two-domain model described above, the four-domain model affords the exploration of the entire parameter space of intrinsic and interaction energies in which the choice of parameter values is, in principle, completely arbitrary. However, an attempt to extrapolate the results of the model

system to real proteins is more grounded if realistic values are used for the thermodynamic parameters governing the intrinsic stabilities and the interaction energies. For this reason, thermodynamic values were used that were derived from the experimentally observed unfolding of isolated helices and entire proteins (20, 22–25), as described in the legend of Figure 2. In essence, the model can be considered a low-resolution depiction of a four-helix bundle protein, wherein the behavior of each state can be considered explicitly.

From the parameters described above, the temperature dependence of the interaction energy term, Δg_{int} , for the four-domain model protein can be calculated (Figure 2A). As expected for a predominantly hydrophobic interaction, a low temperature makes it favorable to break the interactions between different units (i.e., helices) while a high temperature renders it unfavorable. Additionally, at $\sim 73^\circ\text{C}$, the free energy for unfolding into the fully unfolded state (state “Unf”) is zero. As there are no stable intermediates within this temperature region, the unfolding transition is highly cooperative (Figure 2C). Second, at $\sim 40^\circ\text{C}$, the free energy profiles of the fully unfolded state and the intermediate states (states 1–6) cross, the Unf state being more stable at high temperatures and the intermediates being more stable at low temperatures. Although this behavior is a function of the relative energetic parameters of each state, this basic trend is not subject to the limitations imposed by the specific four-domain model used here. As discussed above, the magnitude of ΔC_p for a particular state determines the degree of curvature of the free energy profile. The bulk of the positive ΔC_p of unfolding is due to hydrating apolar surface that is buried in the native state. Thus, states which retain more intramolecular interactions at the expense of solvent contacts give smaller values for ΔC_p and exhibit a more shallow curvature of the free energy profile. Such states belong to a class of compact intermediates in which the least amount of unfolding occurs; that is, this class of compact intermediate would be thermodynamically (and possibly structurally) similar to the native state with respect to the number of intramolecular contacts. Due to the shape and position of the free energy profile, these states are the first to become populated at low-temperature transitions (i.e., states 1 and 2 as defined in Table 2). Transitions to intermediate states exhibiting still fewer intramolecular interactions occur at lower temperatures as determined by the increased curvature of their free energy profiles.

With regard to the high-temperature transition, as no other states are significantly populated, information about states other than the native and fully unfolded states cannot be extracted from high-temperature unfolding experiments. The thermodynamic parameters obtained from fitting of the excess heat capacity data to a two-state model would provide accurate values for complete unfolding. However, the fitted two-state parameters would suggest that the native state is stable by ~ 11 kcal/mol over the denatured state when the free energy is extrapolated back to 25°C (not shown). In fact, the native state is only ~ 7 kcal/mol more stable than the nearest intermediate at this temperature (Figure 2A). If this hypothetical scenario represented a real protein, these intermediates would be the ones accessed through hydrogen exchange measurements, and they would likely be the states most relevant to understanding biological function. This

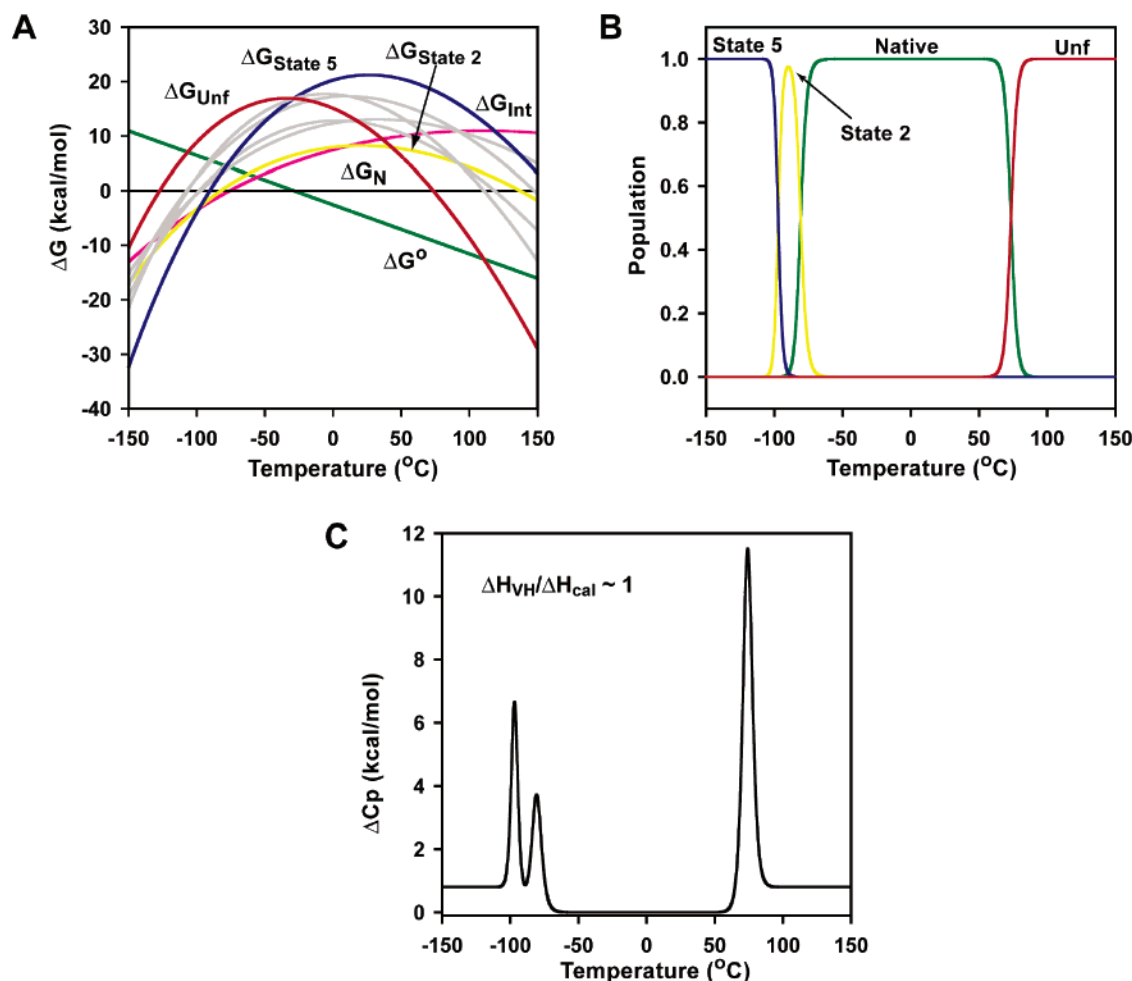


FIGURE 2: Simulated temperature dependence of the four subglobal unit system, as defined in Table 2. Each subglobal unit was modeled as a 20-residue helix and given the following intrinsic thermodynamic parameters: $\Delta H^\circ(25^\circ\text{C}) = 22\text{ kcal/mol}$, $\Delta S^\circ(25^\circ\text{C}) = 90\text{ cal K}^{-1}\text{ mol}^{-1}$, and $\Delta C_p^\circ = 0\text{ cal K}^{-1}\text{ mol}^{-1}$. These parameter values were based upon the experimentally observed values measured for the leucine zipper protein GCN4 (20), for polyalanine helical peptides (22), and for poly(L-lysine) helical peptides (23), as well as the entropy of helix unfolding which is known to be between 4.0 and 5.5 $\text{cal K}^{-1}\text{ mol}^{-1}\text{ residue}^{-1}$ (24, 25). The interaction energy between the subglobal units, Δg_{int} , was calculated from a $\Delta H_{\text{int}}(25^\circ\text{C})$ of -6 kcal/mol , a $\Delta S_{\text{int}}(25^\circ\text{C})$ of $-50\text{ cal K}^{-1}\text{ mol}^{-1}$, and a $\Delta C_{p,\text{int}}$ of $200\text{ cal K}^{-1}\text{ mol}^{-1}$ and is also based upon a previous structural thermodynamic parametrization of GCN4 (20). To simulate the entropic cost of loop closure, the terminal units were assigned the following additional interaction parameters: $\Delta H_{\text{close}} = 0\text{ kcal/mol}$, $\Delta S_{\text{close}}(25^\circ\text{C}) = 16\text{ cal K}^{-1}\text{ mol}^{-1}$, and $\Delta C_{p,\text{close}} = 0\text{ cal K}^{-1}\text{ mol}^{-1}$ (which is the conformational entropy of freezing four residues) (21, 25, 37). Shown in panel A is the relative stability of the various system states. The ΔG of the native state (ΔG_N) is shown as a black line, that of the unfolded state (ΔG_{Unf}) as a red line, the intrinsic stability of each subunit (ΔG°) as a green line, and the ΔG of interaction between each subunit (Δg_{int}) as a magenta line. Data for states 2 and 5 are depicted with blue and yellow lines, respectively. The data for remaining states defined in Table 2 are depicted with gray lines. Shown in panel B are the relative probabilities of the system states and in panel C the simulated change in system heat capacity, $\langle\Delta C_p\rangle$. The cooperativity ratio $\Delta H_{\text{VH}}/\Delta H_{\text{cal}}$ refers to the high-temperature peak, determined as described in ref 2.

difference in free energy between an intermediate state and the unfolded state corresponds to an equilibrium situation in which only one of every 1000 denatured (i.e., non-native) molecules is completely unfolded, while the remaining denatured molecules populate “compact intermediate” states. This simple example highlights the fact that classic high-temperature unfolding experiments can provide very little insight into the states that are accessed by hydrogen exchange.

An additional and nontrivial consequence of fitting the high-temperature transition to a two-state model is that it will predict a cooperative cold denaturation transition at the temperature where the ΔG for the Unf state is zero (i.e., ca. -125°C). The existence of the intermediate states, however, dramatically affects the expected behavior. The simulations

in Figure 2 demonstrate that (1) cold denaturation occurs at temperatures much higher than those predicted by a two-state model, (2) the transition is not cooperative (see Figure 2C), and (3) the final denatured state at a low temperature does not correspond to the final denatured state at a high temperature.

It is important to stress that while the parameter values chosen for the intrinsic stabilities and interaction terms for the four-subglobal unit system were obtained from a structural thermodynamic analysis of a real protein [i.e., the GCN4 leucine zipper peptide (20)], the results of the model do not depend on the structural basis of these values. Using more general thermodynamic parameters, such as those used for the two-domain system [i.e., ΔH° , ΔS° , and ΔC_p° values more typical of globular proteins (26) rather than of a helical

coiled coil], produces the same qualitative features of a cooperative denaturation at high temperatures and a noncooperative unfolding of the protein at low temperatures.

Importance of the Cold-Denatured Intermediates

Inspection of the results of simulations of various models with different configurations (i.e., the numbers of subglobal units, the number of interactions per unit, etc.) reveals that there is no correlation between the cooperative behavior observed during heat and cold denaturation. A transition that is highly cooperative during heat denaturation may or may not unfold cooperatively during cold denaturation. Several general trends, however, do emerge from this analysis. First, cooperativity arises when breaking the interactions between subglobal groups is so unfavorable that only the combined instability of all the subglobal units is sufficient to overcome the stability conferred by the total of all interactions between groups. This observation provides important insight from a mechanistic point of view. The classical view is that denaturation of a protein involves destabilization of the hydrophobic protein core (i.e., decreasing the interaction energies through which smaller structures interact). The hierarchical model suggests, however, that cooperative unfolding occurs only when the interaction energies between units are comparatively high. In fact, according to the parameters used for Figures 1 and 2, the interaction energy can even increase through the transition region. Hence, cooperative unfolding results from a destabilization of the subglobal units. If parameter values are chosen so that the protein is unfolded through destabilization of the interactions between subglobal units (i.e., decreasing Δg_{int}) intermediates accumulate due to the fact that ΔG° is relatively small, and the transition exhibits only marginal cooperativity.

Second, the states that are populated during cold denaturation are thermodynamically relevant to an understanding of the native state ensemble. This point is most clearly demonstrated in Figure 2A. Under conditions of maximum stability of the native state (relative to the U state), many of the possible intermediate states are lower in energy than the completely unfolded state. As such, these are the states that would be accessed through hydrogen exchange experiments, and it is an understanding of these states that would provide insight into the energy landscape of functional proteins. Thus, a structurally resolved view of the cold denaturation process provides an unprecedented opportunity to characterize the dominant conformations in the native state ensemble.

Experimental Access to Cold Denaturation by Solution NMR Spectroscopy

The detailed examination of the structural transitions underlying cold-induced denaturation would seem most suited for solution NMR methods. Unfortunately, characterization of protein cold denaturation by solution NMR methods is frustrated by the fact that the properties of proteins are such that cold denaturation occurs below the freezing point of water. Catastrophic freezing of protein solutions can be avoided to temperatures as low as -20°C with careful supercooling of small sample volumes (27). This is predicted, however, to be insufficiently cold to induce denaturation in stable, native proteins. In addition, the high viscosity of water at these temperatures results in significantly slower tumbling

and correspondingly shorter spin–spin relaxation times (T_2). Short T_2 values severely limit the power and flexibility of multiple-pulse NMR experiments in at least two ways. The signal-to-noise ratio of a Lorentzian line rapidly degrades with a decrease in T_2 , and the effectiveness of the currently available library of multidimensional and multinuclear NMR experiments begins to fail as T_2 approaches the inverse of the coupling constant responsible for coherence transfer. These conditions prevail at the low temperatures required for observation of cold denaturation of stable native proteins.

Historically, destabilizing perturbations such as mutations, chemical denaturants, and hydrostatic pressure have been employed to promote cold denaturation at higher temperatures and, in the case of pressure, to lower the freezing point of water itself (28). However, these adjunct perturbations tend to distort the energy landscape of the native state and can potentially obscure features unique to cold denaturation by compressing the free energy range between the native and non-native states. This can be seen by comparing the experimentally observed dependence of the apparent free energy for unfolding of the subglobal cooperative units of apocytochrome b_{562} on the destabilizing effects of chemical denaturant and hydrostatic pressure (8, 9). Apocytochrome b_{562} is a small four-helix bundle protein (29) that has the thermodynamic signature of the protein molten globule, a small change in heat capacity upon unfolding. In an effort to understand the energetic origin of its unusual structure, native state hydrogen exchange was carried out as a function of chemical denaturant (9) and hydrostatic pressure (8). The cooperative substructures of the protein revealed by the two types of perturbation were the same, leading to the conclusion that they dominate the energy landscape of this protein. These results also illustrate the difficulties that can be introduced into studies seeking to illuminate cooperative units of structure by the simultaneous application of different types of structural perturbation that destabilize the native state. In the case of apocytochrome b_{562} , application of pressure tends to compress the free energy range between the same units of cooperative structure that are revealed by a chemical denaturant. This makes resolution of the individual structural units problematic in much the same way that heat denaturation can mask non-two-state unfolding behavior.

In an effort to escape these limitations, we employed a technology that was originally introduced to alleviate the difficulties in solution NMR spectroscopy introduced by slow molecular tumbling of large proteins. To avoid many of the technical issues of working in highly viscous or frozen solutions at low temperatures and to avoid compromising the clarity of the cold denaturation process by use of adjunct perturbations, we have turned to a novel sample preparation that preserves native-like solution conditions while allowing high-resolution NMR spectroscopy to be carried out at very low temperatures. This is achieved by encapsulating the protein of interest in the protective aqueous environment of a reverse micelle and dissolving the entire particle in a low-viscosity solvent such as liquid propane or ethane (30–32). Preparations of encapsulated proteins dissolved in short chain alkane solvents are stable to temperatures as low as -40°C (14, 33), just within reach of the range anticipated to be required for observation of significant cold-induced structural transitions.

Comparison of spectra of encapsulated proteins and their spectra in free aqueous solution indicates that encapsulation conditions can usually be found that result in the maintenance of native structure (30, 33–35). In the one case examined in detail thus far, the structure of encapsulated ubiquitin was found to be remarkably similar to both the free solution and crystalline states of the protein (36).

The confinement of a protein within the protective shell of a reverse micelle is not without thermodynamic consequences, particularly with respect to stability. Indeed, it has long been appreciated that placement of a protein within a restraining cage will suppress population of more extensive states (37). However, for realistic dimensions, confinement will result in the separation rather than the collapse of the free energy manifold of states. This means that the resolution of states will not be degraded by encapsulation, in contrast to the effects of using hydrostatic pressure or a chemical denaturant to promote cold-induced structural transitions. Furthermore, a simple test for ancillary effects arising from confinement can be made by simply varying the inner volume of the reverse micelle particle (14). In a similar vein, careful variation of the nature of the buffer (pH and ionic strength) and reverse micelle surfactant mixture relieves the concern about significant perturbation of the protein ensemble by protein–surfactant interactions (14, 38).

Cold-induced denaturation of encapsulated ubiquitin has been found to be highly noncooperative and a strictly reversible process (14). The use of low-viscosity solvents such as pentane allows for the use of high-resolution solution NMR methods and affords highly detailed insight into the structural transitions that underlie cold-induced denaturation. The cold denaturation of ubiquitin occurs in a broad temperature range between -20 and -35 °C. Only subtle (though interesting) effects are seen as the temperature is reduced from room temperature to -10 °C. Between -10 and -35 °C, both ^{15}N and ^{13}C HSQC spectra display loss of selective cross-peaks, consistent with these sites being in slow exchange with non-native structures on the NMR chemical shift time scale (from ~ 10 to 10^3 s $^{-1}$). Interestingly, no new cross-peaks are observed, which implies that many non-native structures are populated and are not averaged into a single “unfolded” species. This is not surprising, given the low temperature and corresponding small thermal energy available to the destabilized polypeptide chain. All cross-peaks are reduced in intensity, and those peaks that retain significant intensity do not change their chemical shifts appreciably. This is an important observation. It should be noted that the chemical shift and line width of the encapsulated water resonance indicate that the water remains liquid throughout. Progressive rather than a single globally cooperative transition is indicated. A deeper appreciation of the structural nature of the cold-induced changes in ubiquitin is revealed in Figure 3 which clearly indicates that the structural perturbations induced by low temperatures are not randomly distributed but are strikingly clustered to form a contiguous structural unit. This view is most consistent with the penetration of water into a loosely packed but topologically compact region of the structure rather than the more extensively unfolded polypeptide chain associated with thermally induced unfolding. Qualitatively, these observations are largely what one would anticipate on the basis of the statistical thermodynamic treatment outlined above.

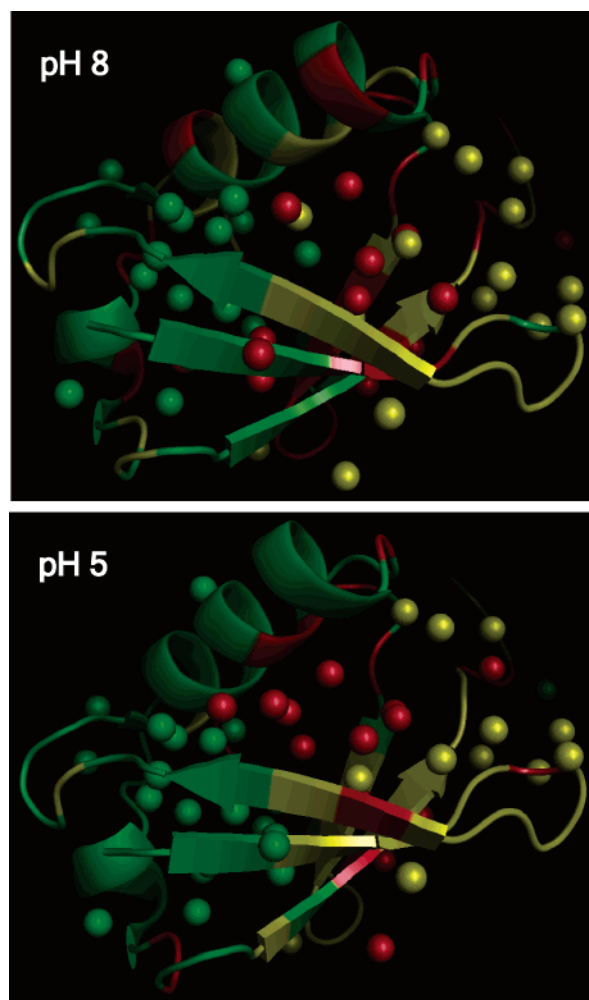


FIGURE 3: Summary of the progressive noncooperative cold-induced structural transitions of ubiquitin observed by heteronuclear NMR spectroscopy (14). Shown is a ribbon representation of the backbone structure of encapsulated ubiquitin (36). Regions with amide NH and C $_{\alpha}$ H resonance chemical shifts of the native structure that have significant intensity are colored green. Those NH sites that are reduced to less than 5% of their initial intensity at -25 and -30 °C are colored yellow and red, respectively. Spheres representing each methyl group in the protein are similarly colored. Results obtained at pH values above (top) and below (bottom) the isoelectric point of the protein (pI ~ 6.8) are summarized and indicate that charge–charge interactions between the anionic head groups of the surfactant have little influence on the cold-induced structural transitions. See also the work of Pometun et al. (38).

Putting them in a quantitative framework requires a more general treatment of the manifold of states.

Dissecting the Cold Denaturation of Ubiquitin Using COREX, a Structure-Based Model of Conformational Fluctuations in Proteins

In studying the nature and energetics of protein structural fluctuations, Hilser and Friere (39) developed the COREX algorithm to model the native state as an ensemble of partially folded conformations (microstates), each of which is derived from the high-resolution structure of the native state and constructed to possess a dual structural–thermodynamic character. In brief, the structure for each microstate is generated by treating local fluctuations as local folding–unfolding reactions that occur in an otherwise folded and nativelike protein. This algorithm generates a large number

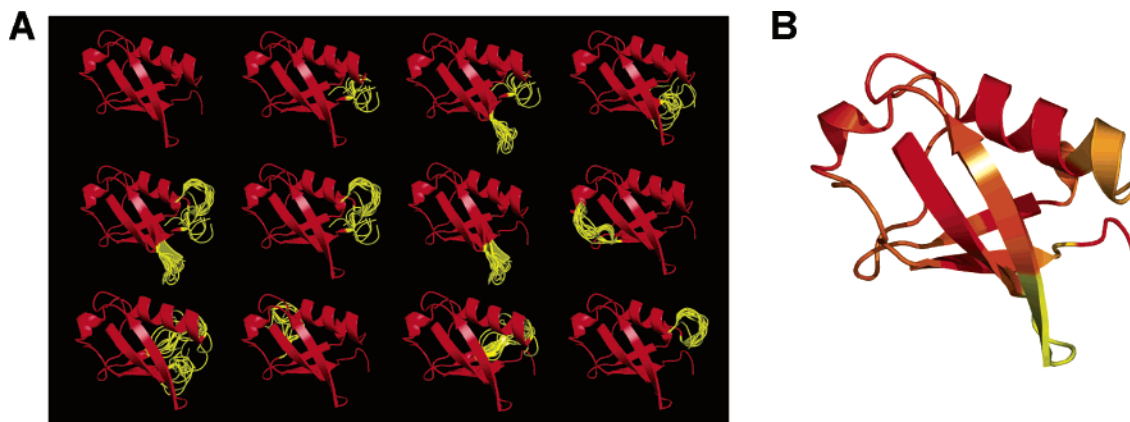


FIGURE 4: (A) Conformational ensemble of ubiquitin as modeled by the COREX algorithm. Shown are the 12 microstates (of $\sim 10^5$ total states in the ubiquitin ensemble) calculated to have the highest probabilities under native conditions. The aggregate sum of the probabilities for these 12 states accounts for 99% of the partition function calculated for ubiquitin [the partition function is defined as the total sum of the statistical weights ($Q = \sum_i K_i$)]. Each microstate exhibits a “dual” structural character and consists of a mixture of regions that are considered to be nativelike (red) and regions that are treated thermodynamically as unfolded (yellow). (B) Time-averaged representation of the ubiquitin ensemble. Residues are color-coded according to the ratio of the summed probability of all states in which a particular residue is folded to the summed probability of all states in which that same residue is unfolded [ratio = $k_j = (\sum_i P_{f,j})/(\sum_i P_{unf,j})$ for each residue j and overall states i]. Residues colored red are stable and fluctuate the least, whereas residues colored yellow fluctuate the most. Molecular diagrams in this figure were made using PyMol (48).

of different microstates through the combinatorial unfolding of a set of predefined folding units. By means of an incremental shift in the boundaries of the folding units, an exhaustive enumeration of partially unfolded states is achieved for a given folding unit size.

The probability of each microstate is estimated using a structure-based calculation with a parametrized energy function that has been calibrated previously and tested extensively (21, 26, 40–46) (see Appendix). Once the free energies are known, the probability of each state in the ensemble can be determined from the Boltzmann relationship:

$$P_i = \frac{K_i}{\sum_i K_i} \quad (5)$$

where the statistical weight of each state (K_i) is determined by the relative Gibbs free energy [$K_i = \exp(-\Delta G_i/RT)$, where R is the gas constant and T is the absolute temperature] and the summation is over all states i in the ensemble.

Given the probabilities of all states, it is then straightforward to compute the relative stability of the different regions of the protein. Within COREX, this is facilitated using a quantity described as the residue stability constant:

$$\kappa_{f,j} = \frac{\sum P_{f,j}}{\sum P_{unf,j}} \quad (6)$$

where the numerator is the summed probability of all states in the ensemble in which a residue is folded and the denominator is the summed probability of all states in which a residue is unfolded (39). Using this approach, the low-energy states in the ubiquitin ensemble (Figure 4A) can be mapped onto the high-resolution structure, providing a single-molecule representation of the conformational fluctuations (Figure 4B). It is important to note, however, that this representation, which is tantamount to mapping the hydrogen exchange rates of each residue onto the structure, provides

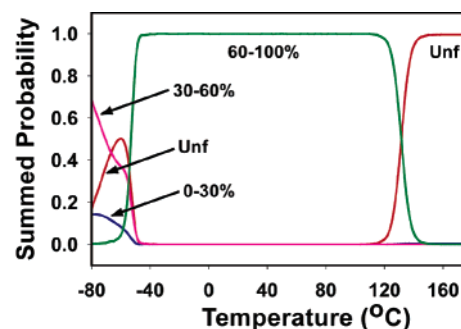


FIGURE 5: Effects of temperature on the ubiquitin ensemble. The ensemble was subdivided on the basis of the amounts of native structure: the fully unfolded state (red), states between 0 and 30% native structure (blue), states between 30 and 60% native structure (magenta), and all states between 60 and 100% native structure (green).

only the average behavior at each residue and little information about the states themselves.

Simulation of the Cold Denaturation of Ubiquitin by COREX

The effect of temperature on the distribution of states in the ubiquitin ensemble can be seen in Figure 5 where the various microstates were grouped according to fraction folded. The fraction folded is the ratio of folded residues in each microstate to the total number of residues of ubiquitin. Of significance is the fact that the COREX algorithm predicts divergent behavior for cold- versus heat-induced unfolding of ubiquitin. Thermal denaturation of ubiquitin at high temperatures is calculated to proceed in a cooperative manner, with the transition dominated by the fully folded native state and the fully unfolded denatured state, with no significant population of structural intermediates throughout the transition. This highly cooperative, heat-induced unfolding behavior calculated for ubiquitin is consistent with what is observed experimentally (47).

In contrast, ubiquitin at low temperatures is predicted to undergo a transition in which intermediate states are sig-

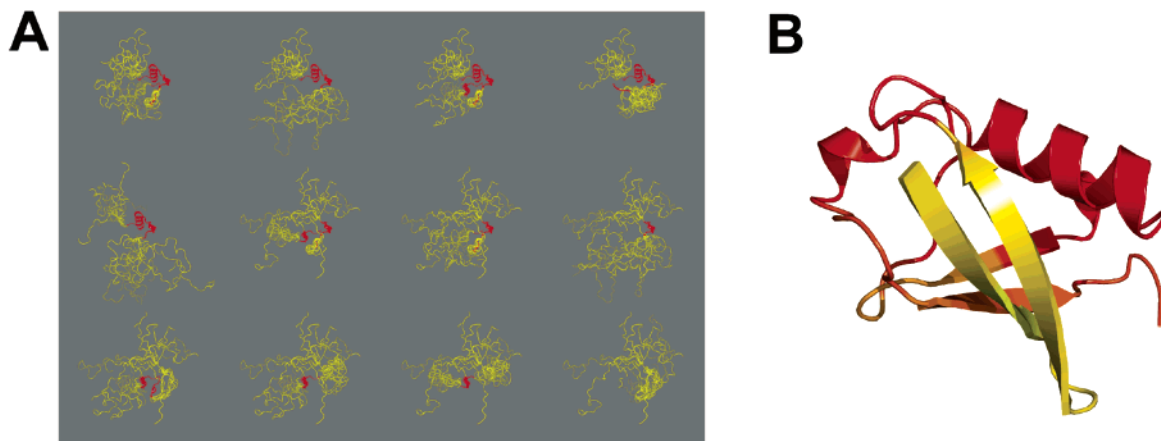


FIGURE 6: (A) Twelve most probable states of the ubiquitin ensemble under low-temperature conditions. The aggregate sum of the probabilities for these 12 states accounts for $\sim 90\%$ of the partition function calculated for ubiquitin at -70°C . (B) Time-averaged representation of the ubiquitin ensemble at low temperatures. All structures are colored according to the same protocol given in Figure 4. Molecular diagrams in this figure were made using PyMol (48).

nificantly populated. Furthermore, these states are predicted to be persistent and stable. The calculated effect of temperature on the ubiquitin ensemble by the COREX algorithm is in qualitative agreement with the unfolding behavior predicted by the hierarchical model presented above, namely, that cooperative thermal denaturation and noncooperative cold denaturation are observed.

The 12 structural thermodynamic states of ubiquitin that possess the greatest probability under native conditions are shown in Figure 4A. For comparison, the 12 most probable states populated at low temperatures are shown in Figure 6A. The dominant state at high temperatures is the fully unfolded state, which is populated by a factor of 10^3 over any other member of the ensemble. In other words, the ensemble at high temperatures can be approximated well by only the fully unfolded state. As can be seen in Figure 6A, however, cold-induced denaturation of the ubiquitin ensemble consists primarily of unfolding of the β -sheet domain, whereas the major α -helix region, including the loops on either side of the helix, remains folded in its nativelike structure. The smaller 3_{10} -helix in ubiquitin is also populated to a non-negligible amount at low temperatures. This is shown more clearly in Figure 6B, where a cartoon of the ubiquitin structure is color-coded according to the probability that a given residue is folded in the cold-denatured ensemble. As in Figure 6A, it is apparent that the major α -helix of ubiquitin remains folded at low temperatures and, to a lesser extent, the region of the protein structure that is defined by the smaller α -helix under native conditions. If the residues calculated to be folded in the most probable states of the cold-denatured ubiquitin ensemble (i.e., residues 19–41 and 49–58 which are colored red in Figure 6B) are defined as a cooperative unit, the interaction surface between this defined cooperative unit and the remainder of the protein consists of approximately 1770 \AA^2 (2) of hydrophobic (apolar) surface and 211 \AA^2 (2) of hydrophilic (polar) surface (including both interfaces). Thus, the COREX calculations are consistent with what was observed by the hierarchical model in which interactions between “subglobal” units are driven mainly by the nonspecific burial of hydrophobic surface.

The results of the hierarchical subglobal model applied to protein cold denaturation presented above suggest that the unfolding of proteins at low temperatures should, in general,

be noncooperative. The results of applying the COREX algorithm to multiple protein folds further support this notion. Shown in panels A and B of Figure 7 are the results of simulating the cold denaturation of cytochrome *c* and staphylococcal nuclease (SNase), respectively. The COREX simulations predict the heat-induced unfolding of both proteins to occur in a more or less globally cooperative manner but to significantly populate partially unfolded states during cold denaturation. In the case of the cytochrome *c* ensemble, states that have residues 1–13 and 86–93 folded are favored at low temperatures (Figure 7C). For SNase, it is the two C-terminal helices that are predicted to remain folded at temperatures below the cold-induced structural transition.

Conclusions

Recent NMR results demonstrate that reversible cold denaturation can provide access to the cooperative substructures of proteins (14). Theoretical modeling of the cold denaturation process reveals the thermodynamic nature of low-temperature states. These states correspond to folded cooperative substructures of proteins that are approximated as cooperative units. Because of the thermodynamics associated with exposing hydrophobic surface, these subglobal units of protein structure do not behave independently at high temperatures. Instead, they become energetically coupled, obscuring the detailed energetic balance within the protein structure that is undoubtedly a fundamental aspect of their functions. It is this detailed energetic picture that cold denaturation can provide, and with the recent methodological advances that provide access to cold denaturation by NMR, researchers can obtain an unprecedented structurally resolved view of the protein ensemble.

Interestingly, the results of the hierarchical model and the COREX analysis reveal that the subglobal units of protein structure need not correspond to classical secondary structural units or structurally defined motifs. It is the balance of all possible interactions between all possible folding units that combines to define the cooperative unit under a given set of conditions. These cooperative boundaries may or may not correspond to structural boundaries.

Finally, the COREX algorithm (39) represents a hybrid structural–thermodynamic model of a protein’s conforma-

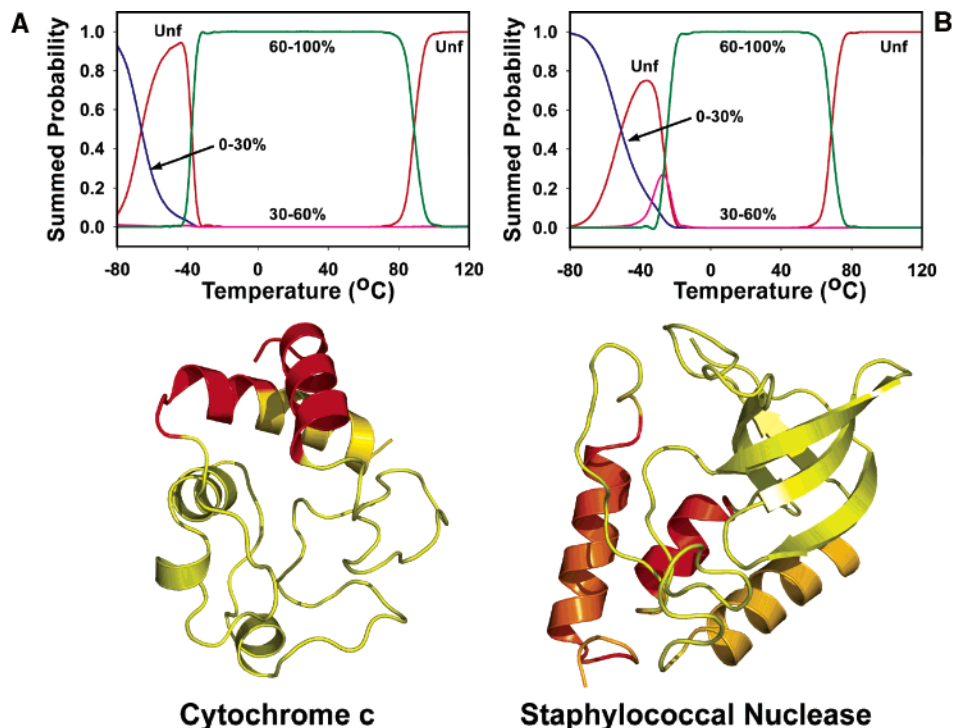


FIGURE 7: Temperature dependence of the horse cytochrome *c* (A) and staphylococcal nuclease (B) ensembles. As in Figure 5, the ensembles for each protein were divided on the basis of the amounts of native structure: the fully unfolded state (red), states between 0 and 30% native structure (blue), states between 30 and 60% native structure (magenta), and all states between 60 and 100% native structure (green). Time-averaged representation of the ensembles of cytochrome *c* and staphylococcal nuclease at low temperatures. Residues colored red are stable and fluctuate the least, whereas residues colored yellow fluctuate the most. Molecular diagrams in this figure were made using PyMol (48).

tional ensemble in which the partially folded states are modeled to have largely the same structural features as those observed by NMR-monitored cold denaturation. For each state in the ensemble, folded segments of the protein are modeled by COREX to retain the same native-like geometry as observed in the high-resolution structure, whereas unfolded segments are modeled as unfolded. In effect, the ensemble is composed of states with a dual character, with some regions being folded and native-like in each state and some regions being unfolded and denatured-like. It is noteworthy that this dual character is precisely what is observed for the ubiquitin intermediates populated during cold denaturation (14). The success of COREX in modeling the cold denaturation of ubiquitin suggests that this algorithm can be used to guide research and more deeply investigate the nature of folding–unfolding intermediates. As a hybrid structural–thermodynamic model of a protein’s conformational ensemble, this algorithm provides a vehicle for projecting the effects of well-established physical properties of peptides onto the behavior of proteins.

Appendix

The COREX algorithm is unique in that it utilizes an energetic parametrization to derive the free energy of each partially unfolded state. In other words, from the measured thermodynamics of unfolding of a database of proteins, COREX infers the unfolding energetics for the intermediate states. Shown below is the current COREX energy function used to generate Figures 4–7. The relative Gibbs free energy for each microstate, ΔG_i , is determined by structure-based parametrization of the intrinsic energetics: $\Delta C_{p,i}$, ΔH_i , and S_i . The heat capacity, $\Delta C_{p,i}$, is known to originate primarily

from changes in hydration and has been parametrized in terms of changes in solvent accessible apolar (ΔASA_{apol}) and polar (ΔASA_{pol}) surface area:

$$\Delta C_{p,i} = \Delta C_{p,\text{apol},i} + \Delta C_{p,\text{pol},i} \quad (\text{A1})$$

and

$$\Delta C_{p,i} = a_{\Delta C_p} \Delta ASA_{\text{apol},i} + b_{\Delta C_p} \Delta ASA_{\text{pol},i} \quad (\text{A2})$$

where $a_{\Delta C_p} = 0.44 \text{ cal mol}^{-1} \text{ K}^{-1} \text{ \AA}^{-2}$ and $b_{\Delta C_p} = 0.26 \text{ cal mol}^{-1} \text{ K}^{-1} \text{ \AA}^{-2}$ (41–43). The enthalpy change, ΔH_i , also scales with accessible surface areas and can be written as

$$\Delta H(60^\circ\text{C})_i = a_{\Delta H} \Delta ASA_{\text{apol},i} + b_{\Delta H} \Delta ASA_{\text{pol},i} \quad (\text{A3})$$

and

$$\Delta H(T)_i = \Delta H(60^\circ\text{C})_i + \Delta C_{p,i}(T - 60^\circ\text{C}) \quad (\text{A4})$$

where T is the temperature, $a_{\Delta H} = -8.44 \text{ cal mol}^{-1} \text{ \AA}^{-2}$, and $b_{\Delta H} = 31.4 \text{ cal mol}^{-1} \text{ \AA}^{-2}$ (40, 41). The entropy change, ΔS_i , includes two contributions, one from changes in solvation and the other from changes in the conformational entropy:

$$\Delta S_i = \Delta S_{\text{solv},i} + \Delta S_{\text{conf},i} \quad (\text{A5})$$

The solvation contribution can be written in terms of the polar and apolar values of ΔC_p if the temperatures at which $\Delta S_{\text{solv},\text{apol}} = 0$ and $\Delta S_{\text{solv},\text{pol}} = 0$ are known ($T_{\text{s,apol}}$ and $T_{\text{s,pol}}$, respectively):

$$\Delta S_{\text{solv},i} = \Delta S_{\text{solv},\text{apol},i} + \Delta S_{\text{solv},\text{pol},i} \quad (\text{A6})$$

and

$$\Delta S(T)_{\text{solv},i} = \Delta C_{p,\text{apol},i} \ln(T/T_{s,\text{apol}}) + \Delta C_{p,\text{pol},i} \ln(T/T_{s,\text{pol}}) \quad (\text{A7})$$

$T_{s,\text{apol}}$ has been shown to be 385 K (21), while $T_{s,\text{pol}}$ has been shown to be 335 K (44). The conformational entropies are calculated by considering three contributions:

$$\Delta S_{\text{conf},i} = \Delta S_{\text{bu-ex},i} + \Delta S_{\text{ex-un},i} + \Delta S_{\text{bb},i} \quad (\text{A8})$$

where $\Delta S_{\text{bu-ex},i}$ is the summed entropy change for all side chains that are buried in the fully folded state and become exposed in a microstate, $\Delta S_{\text{ex-un},i}$ is the summed entropy change of solvent-exposed side chains upon unfolding of the peptide backbone, and $\Delta S_{\text{bb},i}$ is the backbone entropy change for residues that become unfolded in a microstate. The magnitudes of the conformational entropy contributions for each amino acid type have been determined from computational analysis of the probabilities of the different dihedral and torsion angles and are reported elsewhere (44, 45). The temperature-dependent Gibbs free energy for each ensemble state, $\Delta G(T)_i$, is then expressed in terms of the standard thermodynamic equation:

$$\Delta G(T)_i = \Delta H(T)_i - T[\Delta S(T)_{\text{solv},i} + \Delta S_{\text{conf},i}] \quad (\text{A9})$$

REFERENCES

- Lifson, S., and Zimm, B. H. (1963) Simplified theory of the helix-coil transition in DNA based on a grand partition function, *Biopolymers* 1, 15–23.
- Lumry, R., Biltonen, R., and Brandts, J. F. (1966) Validity of 2-state hypothesis for conformational transitions of proteins, *Biopolymers* 4, 917–944.
- Englander, S. W. (2000) Protein folding intermediates and pathways studied by hydrogen exchange, *Annu. Rev. Biophys. Biomol. Struct.* 29, 213–238.
- Bai, Y. W., Sosnick, T. R., Mayne, L., and Englander, S. W. (1995) Protein-folding Intermediates: Native-state hydrogen-exchange, *Science* 269, 192–197.
- SwintKrusse, L., and Robertson, A. D. (1996) Temperature and pH dependences of hydrogen exchange and global stability for ovomucoid third domain, *Biochemistry* 35, 171–180.
- Chamberlain, A. K., Handel, T. M., and Marqusee, S. (1996) Detection of rare partially folded molecules in equilibrium with the native conformation of RNaseH, *Nat. Struct. Biol.* 3, 782–787.
- Radford, S. E., Buck, M., Topping, K. D., Dobson, C. M., and Evans, P. A. (1992) Hydrogen-exchange in native and denatured states of hen egg-white lysozyme, *Proteins: Struct., Funct., Genet.* 14, 237–248.
- Fuentes, E. J., and Wand, A. J. (1998) Local stability and dynamics of apocytochrome b_{562} examined by the dependence of hydrogen exchange on hydrostatic pressure, *Biochemistry* 37, 9877–9883.
- Fuentes, E. J., and Wand, A. J. (1998) Local dynamics and stability of apocytochrome b_{562} examined by hydrogen exchange, *Biochemistry* 37, 3687–3698.
- Itzhaki, L. S., Neira, J. L., and Fersht, A. R. (1997) Hydrogen exchange in chymotrypsin inhibitor 2 probed by denaturants and temperature, *J. Mol. Biol.* 270, 89–98.
- Yang, D. W., and Kay, L. E. (1996) Contributions to conformational entropy arising from bond vector fluctuations measured from NMR-derived order parameters: Application to protein folding, *J. Mol. Biol.* 263, 369–382.
- Li, Z. G., Raychaudhuri, S., and Wand, A. J. (1996) Insights into the local residual entropy of proteins provided by NMR relaxation, *Protein Sci.* 5, 2647–2650.
- Volkman, B. F., Lipson, D., Wemmer, D. E., and Kern, D. (2001) Two-state allosteric behavior in a single-domain signaling protein, *Science* 291, 2429–2433.
- Babu, C. R., Hilser, V. J., and Wand, A. J. (2004) Direct access to the cooperative substructure of proteins and the protein ensemble via cold denaturation, *Nat. Struct. Mol. Biol.* 11, 352–357.
- Freire, E., Murphy, K. P., Sanchezruiz, J. M., Galisteo, M. L., and Privalov, P. L. (1992) The molecular basis of cooperativity in protein folding: Thermodynamic dissection of interdomain interactions in phosphoglycerate kinase, *Biochemistry* 31, 250–256.
- Griko, Y. V., Venyaminov, S. Y., and Privalov, P. L. (1989) Heat and cold denaturation of phosphoglycerate kinase (interaction of domains), *FEBS Lett.* 244, 276–278.
- Brandts, J. F., Hu, C. Q., Lin, L. N., and Mos, M. T. (1989) A simple model for proteins with interacting domains. Applications to scanning calorimetry data, *Biochemistry* 28, 8588–8596.
- Freire, E., and Murphy, K. P. (1991) Molecular basis of cooperativity in protein folding, *J. Mol. Biol.* 222, 687–698.
- Hilser, V. J., Townsend, B. D., and Freire, E. (1997) Structure-based statistical thermodynamic analysis of T4 lysozyme mutants: Structural mapping of cooperative interactions, *Biophys. Chem.* 64, 69–79.
- Thompson, K. S., Vinson, C. R., and Freire, E. (1993) Thermodynamic characterization of the structural stability of the coiled-coil region of the Bzip transcription factor GCN4, *Biochemistry* 32, 5491–5496.
- Baldwin, R. L. (1986) Temperature dependence of the hydrophobic interaction in protein folding, *Proc. Natl. Acad. Sci. U.S.A.* 83, 8069–8072.
- Scholtz, J. M., Marqusee, S., Baldwin, R. L., York, E. J., Stewart, J. M., Santoro, M., and Bolen, D. W. (1991) Calorimetric determination of the enthalpy change for the α -helix to coil transition of an alanine peptide in water, *Proc. Natl. Acad. Sci. U.S.A.* 88, 2854–2858.
- Chou, P. Y., and Scheraga, H. A. (1971) Calorimetric measurement of enthalpy change in isothermal helix-coil transition of poly-L-lysine in aqueous solution, *Biopolymers* 10, 657.
- Privalov, P. L., and Gill, S. J. (1988) Stability of protein-structure and hydrophobic interaction, *Adv. Protein Chem.* 39, 191–234.
- Murphy, K. P., Privalov, P. L., and Gill, S. J. (1990) Common features of protein unfolding and dissolution of hydrophobic compounds, *Science* 247, 559–561.
- Murphy, K. P., Bhakuni, V., Xie, D., and Freire, E. (1992) Molecular basis of co-operativity in protein folding. III. Structural identification of cooperative folding units and folding intermediates, *J. Mol. Biol.* 227, 293–306.
- Skalicky, J. J., Mills, J. L., Sharma, S., and Szyperski, T. (2001) Aromatic ring-flipping in supercooled water: Implications for NMR-based structural biology of proteins, *J. Am. Chem. Soc.* 123, 388–397.
- Nash, D. P., and Jonas, J. (1997) Structure of the pressure-assisted cold denatured state of ubiquitin, *Biochem. Biophys. Res. Commun.* 238, 289–291.
- Feng, Y., Sligar, S. G., and Wand, A. J. (1994) Solution structure of apocytochrome b_{562} , *Nat. Struct. Biol.* 1, 30–35.
- Wand, A. J., Ehrhardt, M. R., and Flynn, P. F. (1998) High-resolution NMR of encapsulated proteins dissolved in low-viscosity fluids, *Proc. Natl. Acad. Sci. U.S.A.* 95, 15299–15302.
- Wand, A. J., Babu, C. R., Flynn, P. F., and Milton, M. J. (2003) NMR spectroscopy of encapsulated proteins dissolved in low viscosity fluids, *Biol. Magn. Reson.* 20, 121–160.
- Peterson, R. W., Lefebvre, B. G., and Wand, A. J. (2005) High resolution NMR studies of encapsulated proteins in liquid ethane, *J. Am. Chem. Soc.* 127, 10176–10177.
- Peterson, R. W., Pometun, M. S., Shi, Z., and Wand, A. J. (2005) Novel surfactant mixtures for NMR spectroscopy of encapsulated proteins dissolved in low viscosity fluids, *Protein Sci.* 14, 2919–2921.
- Lefebvre, B. G., Liu, W., Valentine, K. G., and Wand, A. J. (2005) NMR spectroscopy of proteins encapsulated in a positively-charged surfactant, *J. Magn. Reson.* 175, 158–162.
- Shi, Z., Peterson, R. W., and Wand, A. J. (2005) New reverse micelle surfactant systems optimized for high resolution NMR spectroscopy of encapsulated proteins, *Langmuir* 21, 10632–10637.

36. Babu, C. R., Flynn, P. F., and Wand, A. J. (2001) Validation of protein structure from preparations of encapsulated proteins dissolved in low viscosity fluids, *J. Am. Chem. Soc.* 123, 2691–2692.
37. Zhou, H. X., and Dill, K. A. (2001) Stabilization of proteins in confined spaces, *Biochemistry* 40, 11289–11293.
38. Pometun, M. S., Peterson, R. W., Babu, C. R., and Wand, A. J. (2006) Cold denaturation of encapsulated ubiquitin, *J. Am. Chem. Soc.* (in press).
39. Hilser, V. J., and Freire, E. (1996) Structure-based calculation of the equilibrium folding pathway of proteins. Correlation with hydrogen exchange protection factors, *J. Mol. Biol.* 262, 756–772.
40. Xie, D., and Freire, E. (1994) Structure-based prediction of protein-folding intermediates, *J. Mol. Biol.* 242, 62–80.
41. Murphy, K. P., and Freire, E. (1992) Thermodynamics of structural stability and cooperative folding behavior in proteins, *Adv. Protein Chem.* 43, 313–361.
42. Gomez, J., Hilser, V. J., Xie, D., and Freire, E. (1995) The heat-capacity of proteins, *Proteins: Struct., Funct., Genet.* 22, 404–412.
43. Habermann, S. M., and Murphy, K. P. (1996) Energetics of hydrogen bonding in proteins: A model compound study, *Protein Sci.* 5, 1229–1239.
44. D'Aquino, J. A., Gomez, J., Hilser, V. J., Lee, K. H., Amzel, L. M., and Freire, E. (1996) The magnitude of the backbone conformational entropy change in protein folding, *Proteins* 25, 143–156.
45. Lee, K. H., Xie, D., Freire, E., and Amzel, L. M. (1994) Estimation of changes in side chain configurational entropy in binding and folding: General methods and application to helix formation, *Proteins* 20, 68–84.
46. Luque, I., Mayorga, O. L., and Freire, E. (1996) Structure-based thermodynamic scale of α -helix propensities in amino acids, *Biochemistry* 35, 13681–13688.
47. Wintrode, P. L., Makhataдзе, G. I., and Privalov, P. L. (1994) Thermodynamics of ubiquitin unfolding, *Proteins: Struct., Funct., Genet.* 18, 246–253.
48. DeLano, W. L. (2002) *PYMO*L, DeLano Scientific, San Carlos, CA.

BI060855+